2019 6th International Conference on Electric Vehicular Technology (ICEVT)
November 18-21, 2019, Bali, Indonesia

The Effect of Vehicle Inertia on Regenerative Braking Systems of Pure Electric Vehicles

Joga Dharma Setiawan
Mechanical Engineering Department
Universitas Diponegoro
Semarang, Indonesia
National Center for Sustainable Transportation Technology, Indonesia
joga.setiawan@ft.undip.ac.id

Bentang Arief Budiman
Faculty of Mechanical and Aerospace Engineering
Institut Teknologi Bandung, Indonesia
National Center for Sustainable Transportation Technology, Indonesia
bentang@ftmd.itb.ac.id

Ismoyo Haryanto
Mechanical Engineering Department
Universitas Diponegoro
Semarang, Indonesia
National Center for Sustainable Transportation Technology, Indonesia
ismoyo2001@yahoo.de

Munadi
Mechanical Engineering Department
Universitas Diponegoro
Semarang, Indonesia
National Center for Sustainable Transportation Technology, Indonesia
muna_096@yahoo.com

Mochammad Ariyanto
Mechanical Engineering Department
Universitas Diponegoro
Semarang, Indonesia
National Center for Sustainable Transportation Technology, Indonesia
mochammad_ariyanto@ft.undip.ac.id

Mohammad Alfian Hidayat
Mechanical Engineering Department
Universitas Diponegoro
Semarang, Indonesia
alfianhidayat9@gmail.com

***Abstract*—Electric vehicles have the advantage of regenerative braking in which the electric motor can be used as a generator to convert the kinetic energy of a moving vehicle into electrical energy during the braking process. The purpose of this study is to determine the effect of vehicle inertia on the voltage and electrical power profiles at the ultracapacitors as the energy storage system (ESS) and the vehicle speed during the motoring and the generating modes. In this study, an induction motor is used. The combination of regenerative and mechanical braking systems is regulated by the control logic to meet the driver's request. The mathematical model of a regenerative parallel braking system is coded in MATLAB/Simulink. The simulation results show the profiles of electric power flow, energy flow, mechanical braking torque, braking torque by the motor, and the State of Charge (SOC) of the ultracapacitor stacks.**

Keywords— regenerative braking, SOC, ultracapacitors, flywheel, generating mode

I. INTRODUCTION

Electric vehicles have the advantage of regenerative braking. An electric motor which is usually used as a driver can be used as a generator to convert the kinetic energy of a vehicle into electrical energy during the braking process, rather than removing heat energy. This electrical energy can then be stored in energy storage systems (eg batteries or ultracapacitors) and then released to electric motors as driving vehicles.

Regenerative braking must operate safely and effectively, therefore the regenerative and mechanical braking system must be fully integrated. This integration requires a combination of regenerative and mechanical braking to be controlled smoothly and accurately to meet the driver's demand.

Regenerative braking torque settings are carried out using control algorithms and vector control for induction motors. In overcoming the problem of setting braking torque separately from the driving force of the pedal by using a reduction in pressure on the brake booster to regulate the amount of mechanical torque developed by the braking system

II. METHODS OF REGENERATIVE BRAKING

A. Parallel Regenerative Braking

During parallel regenerative braking, both the electric motor and the mechanical braking system always work in parallel (together) to slow the vehicle down shown in Fig. 1 [1]. Because mechanical braking cannot be controlled independently of the brake pedal force, this changes part of the kinetic energy of the vehicle into heat, not electrical energy. The regenerative braking force developed by the electric motor is a function of the hydraulic pressure of the master cylinder, and therefore a function of vehicle deceleration. Because the regenerative braking force available is a function of motor speed and because almost no kinetic energy can be recovered at low motor speed, the regenerative braking force at high vehicle deceleration is designed to be zero so as to maintain braking balance. The parallel braking system does not need an electronically controlled mechanical brake system. A pressure sensor senses the hydraulic pressure in the master cylinder, which represents the deceleration demand. The pressure signal is regulated and sent to the electric motor controller to control the electric motor to produce the demanded braking torque. This is not the most efficient regenerative braking method. However, parallel regenerative braking does have advantages because it is simple and cost-effective. For the use of this method, the mechanical braking system requires a little modification and the control algorithm for the electric motor can be easily

implemented into the vehicle. This method also has the added advantage of always having a mechanical braking system as a backup in the event of a regenerative braking system failure.

B. Four-Quadrant Operation

Many applications require settings for starts and stops from DC motors as in robotic actuation. Consider that the engine operates at a stable speed and is desirable to bring the speed to zero, there are 2 ways to achieve this, namely:

1. Cut off the armature to the engine and let the rotor reach zero speed.

2. The machine can be made to work as a DC generator, thus the stored kinetic energy can be effectively transferred to the source. Storage of this energy and quickly bring the engine to zero speed.

While the cut off in the supply will result in irregular speed responses, the second method provides controlled braking from the engine. To make the engine operate in motor (motoring) mode to go to generating mode, what needs to be done is to reverse the flow of power from the engine to the source power supply. This mode of operation is called regenerative braking. Braking is done by regeneration which means that negative torque is produced in the engine as opposed to positive motor torque. Therefore, the mirror reflection of the torque-velocity characteristics in quadrant I is required in quadrant IV for regeneration, shown in Fig. 2. The first and fourth quadrants are for one direction of rotation, say, forward motoring (FM) and forward regeneration (FR) [2].

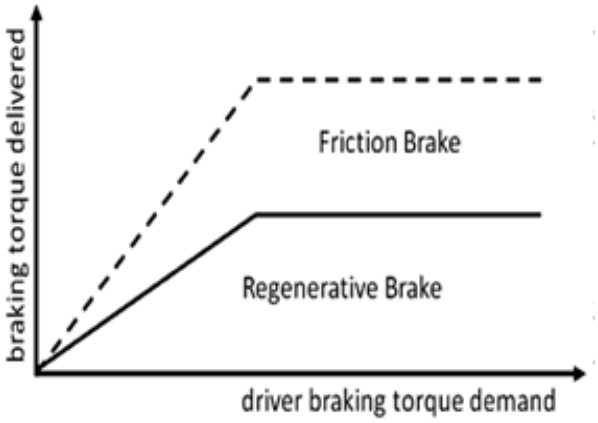

Fig. 1. Parallel regenerative braking strategy [1]

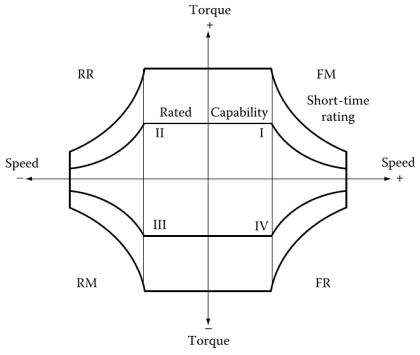

Fig. 2. Four-quadrant torque-speed characteristics [2]

Some applications, such as drive drives in machine tools, require operation in both rotation directions. In this case, quadrant III signifies reverse motoring (RM) and quadrant II, reverse regeneration mode (RR). A motoring and regeneration capable motorbike in both rotation directions is called a four-quadrant variable speed drive (four-quadrant variable speed drive). The torque-velocity characteristics of a four-quadrant drive motor are shown in Fig. 2. The image contains two characteristics, one for rated operating conditions and the other for short-time operations. Short-time characteristics are used for engine acceleration and deceleration and can typically cover 50% -200% greater than rated torque.

C. Three Phase Motor Controller

A three-phase inverter is used to convert DC power into three-phase AC frequency variables using pulse width modulation (PMW). This circuit consists of six power switching devices (power transistors) with a snubber circuit and a feedback diode in a three-phase bridge shown in Fig. 3. The current to the motor is controlled by pulse width modulation using a digital signal processor (DSP). DSP is a special microprocessor specifically designed to support digital signals, common for real-time computing. This can convert the analog feedback signal back into a digital signal to be processed and then convert this digital signal back to the analog signal to switch to the system [5].

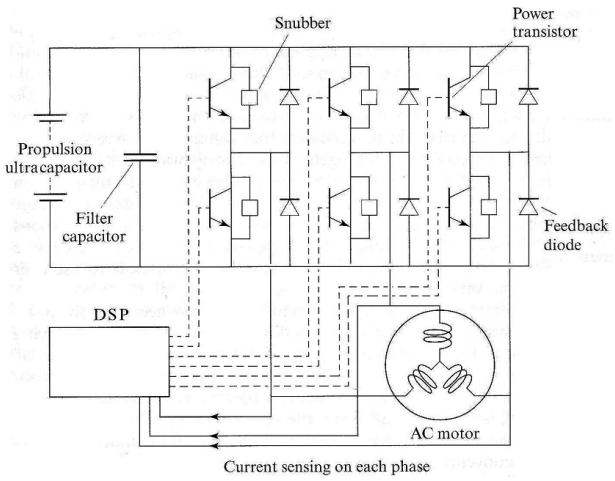

Fig. 3. Induction motor drive circuit [4]

DSP uses vector control as described below to control pulse width, frequency, and phase currents by issuing a signal to the inverter power switch. This will optimize the alternating current output sent to each motor phase. Fast diode feedback is connected in parallel with each power transistor and provides a return path for motor current when the power transistor is off. Snubber circuits control the switching waveforms and suppress electrical transients. There are also bank filter capacitors that are connected to inputs from DC sources. The function of a bank capacitor is to filter the DC input voltage and to provide a low impedance path for high-frequency currents generated during PWM switching [3].

III. VIRTUAL MODELING

The prototype system uses a flywheel to simulate vehicle inertia, which is connected to a three-phase AC induction motor with suitable power electronics, vector control, and ESS to enable regenerative braking and flywheel acceleration as shown in Fig. 4.

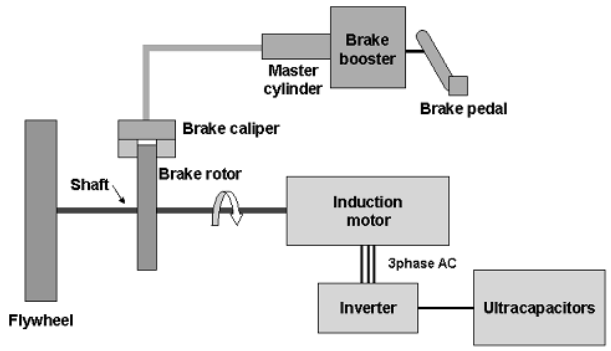

Fig. 4. Prototype configuration [6]

There are two inputs for the system and four main systems. The first input is the accelerator pedal. This input sends a signal to the controller (*Acc*) which determines the amount of torque of the electric motor (T_{elec_req}) required from the electric motor system using a value of 0 or 1 (off/on) as an input for the switch on the ultracapacitor on the electric motor system. The electric motor system then produces torque (T_{elec}) which drives the flywheel. After the flywheel is accelerated to a certain speed, the brake input (F_p) can be applied. This signal, together with the flywheel angular velocity (ω) and the state of charge (SOC), is used in the controller to distribute the braking force between the electric motor system and the mechanical system (T_{mech_req}). The braking torque of a mechanical system (T_{mech}) is then combined with the braking torque of the electric motor system (T_{elec}) to produce the total torque applied to the flywheel ($T_{total} = T_b$). The description of the simulation system for modeling regenerative braking systems and mechanical braking is shown in Fig. 5.

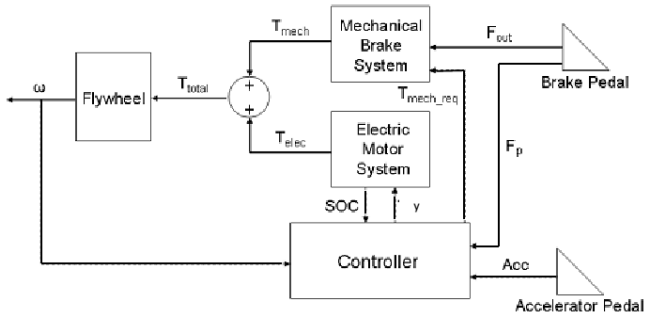

Fig. 5. Modeling scheme [6]

The simulation time range is set to 10 seconds to allow acceleration to an adequate flywheel speed and braking sequence to stop the system. In the first seven seconds, the motor connected to the flywheel accelerated, the brake pedal began to be pressed at t = 7 seconds.

A. Mechanical Brake System

The mechanical braking system shown in Fig. 6 has two inputs: one is the brake force produced by the pedal (F_{out}) and the other is the requested torque control signal (T_{mech_req}) from the mechanical braking controller. The mechanical braking controller uses valve 1 and valve 2 to vary the drive made by the brake booster (F_{boost}). The mechanical braking controller uses the master cylinder pressure as feedback when controlling the boost made by the brake booster.

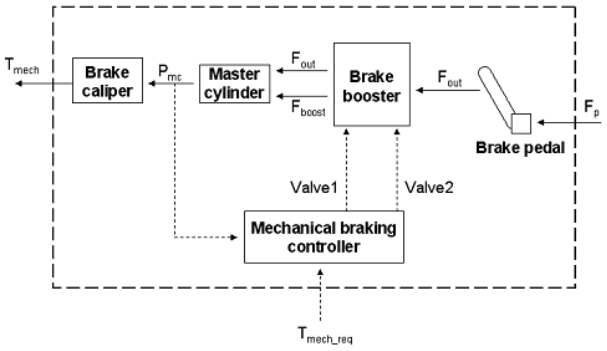

Fig. 6. Mechanical braking system scheme [6]

The air in the brake booster is considered to be an ideal gas undergoing isothermal expansion or compression, which results in the pressure in each chamber being related to the mass of air in the chamber and the diaphragm motion using Equation 1-4 [7].

$$F_{boost} = \left(P_a - P_v\right) A_d \tag{1}$$

$$\begin{aligned} P_v &= \frac{m_{av} RT}{\left(V_{vo} - A_d x_{mc}\right)} \\ P_a &= \frac{\dot{m}_{aa} RT}{\left(V_{ao} - A_d x_{mc}\right)} \end{aligned} \tag{2}$$

$$\dot{m}_{aa} = \begin{cases} C_{aa}\left(P_{atm} - P_a\right) & \text{apply} \\ C_{av}\left(P_v - P_a\right) & \text{release} \\ 0 & \text{hold} \end{cases} \tag{3}$$

$$\dot{m}_{av} = \begin{cases} C_{vm}\left(P_v - P_{acc}\right) & \text{apply} \\ C_{av}\left(P_a - P_v\right) & \text{release} \\ 0 & \text{hold} \end{cases} \tag{4}$$

For the master cylinder, Equation 5 is used as the transfer function [8].

$$\frac{P_{mc}(s)}{X(s)} = \frac{\beta_{mc} A_{mc} / V_{mc}}{s} \tag{5}$$

In this study the braking conditions are applied; thus, all variables are defined in Table 2. The mechanical braking

torque can be calculated from the master cylinder pressure and a review of the time constant (τ_b). The model of mechanical braking torque in the brake caliper subsystem is given by the transfer function in Equation 6 [9].

$$\frac{T_b(s)}{P_{mc}} = \frac{\mu_{pad} A_{caliper} r_{caliper}}{\tau_b s + 1} \quad (6)$$

The mechanical braking torque coupled with braking torque from the electric motor system will produce the total braking. From Equation 7, the value of the flywheel angular velocity (ω) is used as the parameter of regenerative braking [6].

$$T_{mech} + T_{elec} = T_b = J\alpha \quad (7)$$

$$\frac{T_b}{J_{em}} = \alpha \quad (8)$$

However, if we consider an electric vehicle, the rotational speed of the motor connected to the rotation speed of the tire by G, $\omega_w = \omega_m / G$ can be concluded

$$J = \frac{m_e r_d^2}{G^2} \quad (9)$$

where J is the rotational inertia equivalent to a vehicle with an equivalent mass of me. The parameters of the vehicle model used for the simulation are shown in Table 1 [10].

B. Electrical System Modeling

The power electronics system consists of three main components: induction motor, inverter, and ultracapacitor stack. The ultracapacitor stack is used as an energy storage system. While the inverter to convert the current directly into three-phase alternating current to turn on the motor. The scheme of power electronics is shown in Fig. 7.

TABLE I. VEHICLE SPECIFICATIONS

Vehicle equivalent mass (m_e)	m_{e1}	785 kg
	m_{e2}	815 kg
Overall gear ratio (G)		6.67
Wheel radius (r_c)		0.353 m

The reason for the use of ultracapacitors is that they have a high energy storage capacity and better charging-discharging ability to utilize the excess energy produced during braking. Because of its high energy density, the battery can also be used as a storage element. But the problem arises because the charging and discharging processes that are very often can affect battery life [14]. Compared to batteries, ultracapacitors have high power density, better service life but have a lower energy density, during acceleration and braking, it avoids sudden and sudden discharging [15], and ultracapacitors have a wide operating temperature range [16].

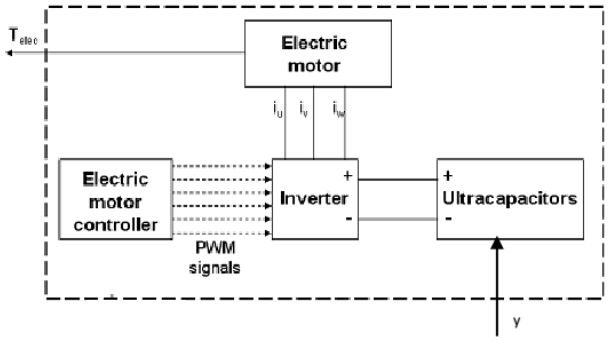

Fig. 7. Power electronics system scheme [6]

To simulate an induction motor, Simulink's asynchronous machine has been determined. Squirrel cage rotor and input in the form of angular velocity have been selected, for the parameters of the induction motor using an induction motor type from BALDOR ZDWNM3611T with motor specifications shown in Fig. 9. Traditionally, DC motors are widely used for traction purposes because of their easy speed control and torque variations that match speed. But now the induction motor seems to be the best engine for propulsion applications, because of its high reliability, strong construction, low maintenance, ability to operate in a hostile environment, and low cost compared to high-power permanent magnet motors that have expensive prices with different efficiency of motor performance is 2% (91% induction motor and 93% BLDC motor) [17]. In addition, motor control and protection have become easier with recent developments in power electronics and control systems [18].

The ultracapacitor stack is modeled using the series resistor-capacitor branch from the Simulink library The assumption used in the study of the combined ultracapacitor voltage value is 385 V and the capacitance is 1 F, the assumption is that it can produce more stored energy.

C. Control System Modeling

The control system is used to distribute and combine torque from the mechanical braking system and a regenerative braking system. The system uses three different controllers. The overall controller of the torque required between the mechanical and regenerative braking system, the mechanical brake control system and the electric motor system in which there is vector control as electric motor control. This system description is shown in Fig. 8.

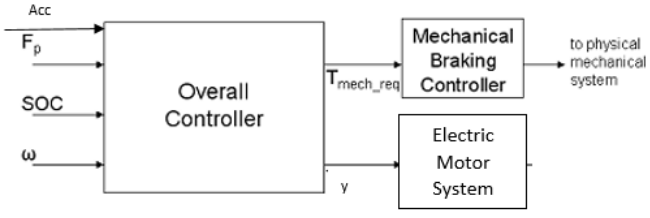

Fig. 8. Control system scheme [6]

The system created by the author is a parallel regenerative braking scheme with the reason being the best economic strategy and the best safety strategy since 1999 [11], and providing easy implementation without other hardware that needs to be added differently with the series regenerative braking strategy required by sensor assembly and modified brake equipment so that it will add to the cost of fulfillment and complexity [13]. Parallel regenerative braking system developed in Matlab/Simulink with the amount of regenerative braking under the amount of mechanical braking.

These four inputs can then be used to calculate the following input into the Stateflow control diagram:

- Driver brake torque demand (M_{demand}) which is proportional to F_p by converting to mechanical braking torque with a look-up table.
- Maximum available regenerative braking torque (M_{max_regen}) which is proportional to ω.
- Ultracapacitor state of charge (U_{SOC}) which is comparable to SOC.
- The angular speed of the electric motor (ω_{motor}) which is equal to the flywheel angular velocity.
- Driver acceleration request (Acc) is used to activate motoring mode.

Two outputs are used to distribute braking torque between mechanical and regenerative brakes and are listed below:

- Requested mechanical braking torque (T_{mech_req}).
- On/off value for switches on ultracapacitor (y).

The 'Brake' status consists of four different substrates that can transition between each substrate depending on the conditions of the input to the Stateflow control system. The four substrates are as follows:

- Standard Substrate (Mechanical and regenerative braking work together)
- Regen only Substrate (Braking is entirely done by regenerative braking)
- Friction only Substrate (kinetic energy produces no voltage to be put back into the energy storage system)
- SOC high Substrate (state of charge of the energy storage system is above a predetermined value and only mechanical braking is active).

The purpose of the mechanical brake controller is to control the torque produced by the mechanical brake system so that it will follow the torque received from the overall controller in the Stateflow control chart (Fig. 9). This controller fully opens valve 1 if the master cylinder pressure (P_{mc}) is 20 percent greater than the demand for brake line pressure (P_{demand}) and fully opens valve 2 if the demand for brake line pressure (P_{demand}) is 20 percent greater than the pressure of the master cylinder (P_{mc}) By using these proportional control valves, the system can follow the requested brake line pressure more accurately. The description of the PID control scheme is shown in Fig. 11.

The mechanical brake controller converts the required mechanical torque signal (T_{mech_req}) to the appropriate demand for brake line pressure (P_{demand}) using the look-up table.

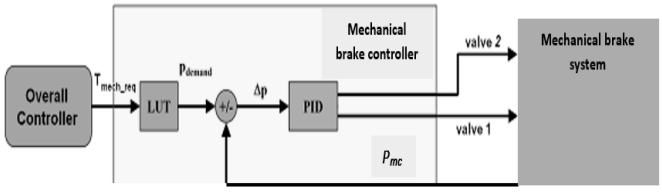

Fig. 9. PID control scheme [6]

The purpose of the electric motor controller is to control the actual speed of the output of the three-phase AC induction motor so that it will follow the speed received from the overall controller.

System design and modeling are done to show the speed control condition of the three-phase induction motor on the inverter to be controlled using the PID controller. Modeling the motor speed control system using an inverter with a PID controller as shown in Fig. 10. From the ultracapacitor voltage source, it is used as input to the inverter so that it can be converted into AC voltage with adjustable frequency adjustments to rotate the three-phase induction motor. The actual speed of the induction motor is then compared to the reference speed, the difference from the motor speed ratio is fed back to the PID controller.

The output of the PID controller goes into the vector control, together with the actual current (I_{abc}). From the vector control, the reference current (I_{abc} reference) is obtained, then the actual current and reference current are

used as inputs to the current control hysteresis to generate pulses. This pulse is used as a trigger for setting the ignition of six Insulated Gate Bipolar Transistors (IGBT) on the inverter. The timing of the frequency ignition process used to adjust the rotation of the induction motor used.

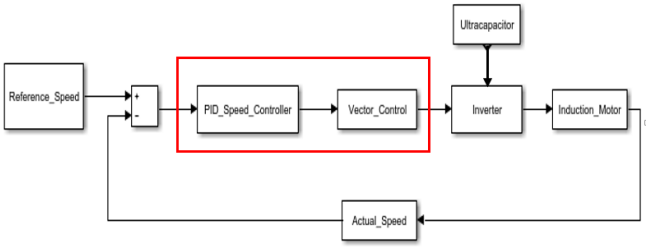

Fig. 10. Block diagram of an electric motor controller for an induction motor [12]

IV. SIMULATION RESULT AND ANALYSIS

The final modeling results are shown in Fig. 11, Simulation parameters are carried out for 10 seconds with ode45 Solver.

The regenerative control system subsystem contains a mechanical braking system (brake booster, master cylinder, brake caliper) along with a flywheel, mechanical brake controller, Stateflow control chart, with a signal source in the form of two Signal Builder blocks containing brake pedal and acceleration pedals. As shown in Fig. 12.

The state-flow control chart consists of four substrates in the Brake status and the addition of Motor Status that occurs when the acceleration signal is more than zero. The transfer from each substrate to the other substrate follows the

conditions of the two-block Signal Builder style brake pedals and accelerator pedals, where the displacement time is adjusted to the PID control found in the vector control

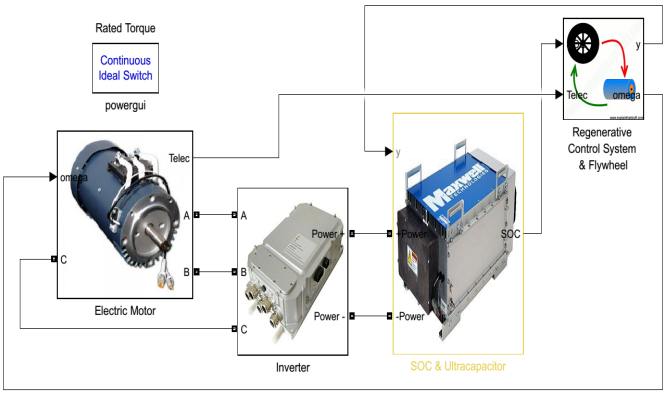

Fig. 11. Final modeling

subsystem. Fig. 13 shows the modeling of Stateflow control chart.

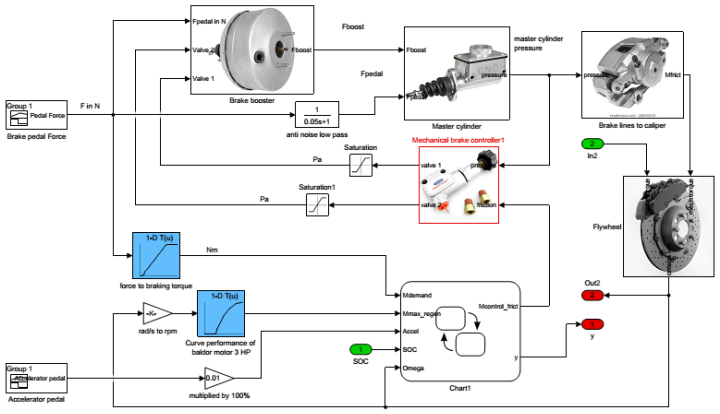

Fig. 12. Sub system regenerative control system and flywheel

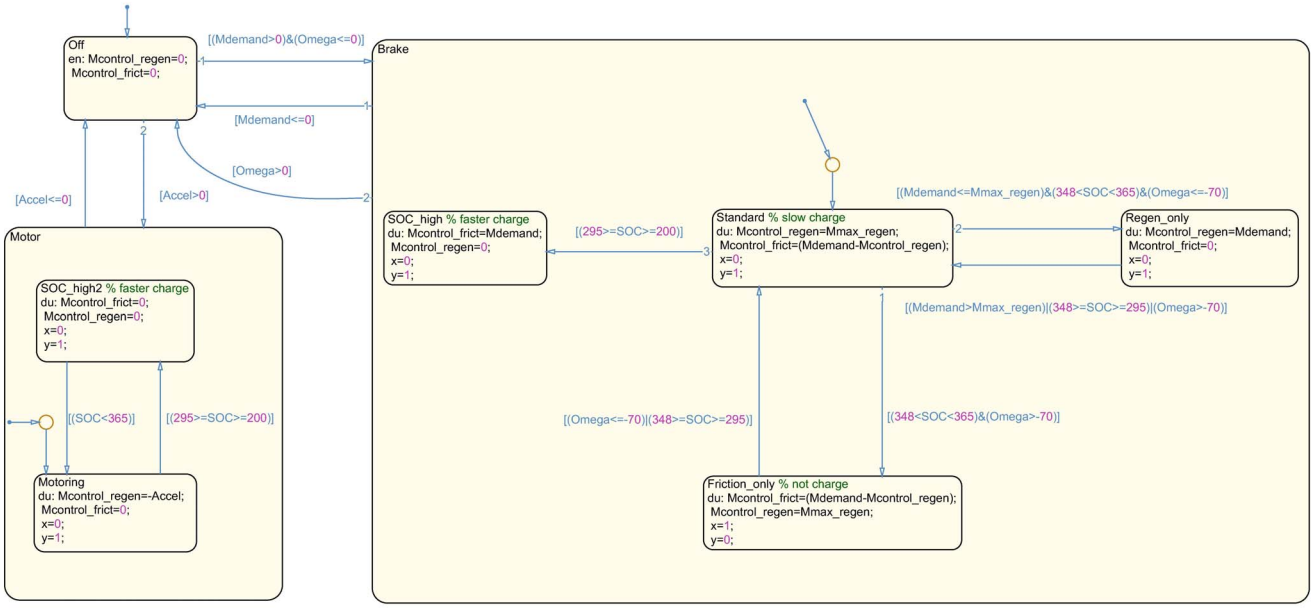

Fig. 13. Stateflow control chart

In carrying out the simulation value is needed for the variables contained in the regenerative control system sub-system. The following Table 2 shows the simulation variables of this study. The variation of the value of the *J* polar inertia moment in the flywheel parameter is based on Table 1 using Equation 9.

Simulation results are used to show the benefits of regenerative braking efficiency using the regenerative braking system. The results also show system functionality to distribute braking force between mechanical and regenerative braking systems, using parameter requirements in the study. In this subchapter, the simulation uses the equivalent mass of vehicle 1 provided in Table 1.

One of the most important outcome parameters for regenerative braking simulations is the voltage from the U_{SOC} ultracapacitor stack which shows the SOC state of charge from the ultracapacitor. At the beginning of the simulation, the ultracapacitor stack voltage at 0 seconds is around 385 V. During the acceleration process it exponentially decreases to create motoring modes from t = 0 s to t = 6.8 s requiring energy from ultracapacitor, consequently the ultracapacitor voltage drops to 119.8 V at t = 6.8 s. When the acceleration pedal is released at t = 7 s, the ultracapacitor starts to increase linearly from the flywheel kinetic energy so that the electric voltage rises from 119.8 V to 154.2 V at t = 8 s. This process is called generating mode as shown in Fig. 14, where the equivalent mass of the vehicle used is me1 as in Table 1.

During regenerative braking (fashion generating) shown in Fig. 15, the flux control current remains constant, seen from t = 6 s to t = 6.8 s with the value of electric current around ± 16 A. The motoring mode transition into generating mode causes the stator flux speed rotates to be less than the motor speed, resulting in a negative slip. This causes an increase in the three-phase current of the motor at t = 6.8 s to t = 7.4 s and the motor changes to the generating mode function. At t = 6.8 s the three-phase current value is ± 16 A

and at t = 7.4 s increases to around ± 49 A, which is then inserted into the ultracapacitor to increase the value of the electric voltage ($SOC_{ucaps} = U_{SOC}$). This simulation is also used to evaluate how the regenerative braking system reacts when the M_{demand} value is greater than M_{max_regen}. This condition occurs when the brake pedal signal starts at t = 7 s or the flywheel angular velocity value is below 70 rad/s. At t = 7 s until t = 8.4 s on Stateflow, it is in the Standard Substrate. When the braking force signal value reaches a maximum of 200 N when t = 7.5 s causes the motor three-phase current to decrease starting at t = 7.5 s until at t = 8 s with a current value of ± 20 A.

In Fig. 16 at t = 8.4 s until t = 10 s in Stateflow is in Friction only Substrate. Ideal switches are added to the system which will make the circuit open or closed with an ultracapacitor stack when the flywheel angular velocity is below 70 rad/s. In this condition, electrical energy cannot get out of the ultracapacitor stack and vice versa.

Another interesting parameter in the regenerative braking process is the flow of power from and to the ultracapacitor stack. Displayed in Fig. 18 simulation with J_{em1} value = 2.19715 kg.m^2. The minimum point of the electric power profile on the ultracapacitor stack P_{ucaps} min (t = 1.14 s) = 14.12 kW while at t = 6.68 s the curve tends to increase from -1.849 kW to the maximum P_{ucaps} point (t = 7.94 s) = 2.94 kW. A negative value on electric power means that the electric power flows from the ultracapacitor stack to the motor to drive the flywheel or called motoring mode and a positive value on electric power means the motor is in generating mode or which means the electric power flows from the motor to the ultracapacitor stack.

Fig. 15 shows the profile of energy stored during the braking process. At t = 0 s to t = 6.74 s the energy on the ultracapacitor decreases because the motor in the motoring mode, i.e. the energy stored in the ultracapacitor stack (E_{ucaps}) is used to move the motor during the acceleration process. The energy reduction from E_{ucaps} initial (t = 0 s) = 20.59 Wh to E_{ucaps} min (t = 6.74 s) = 1.992 Wh occurs in motoring mode. At t = 6.74 s to 7.08 s is a transition into generating mode, on E_{ucaps} (t = 7.08 s) = 2.188 Wh there is an increase in energy to max E_{ucaps} (t = 8.24 s) = 3.368 Wh. This increase in energy is due to the motor in generating mode.

TABLE II. SIMULATION VARIABLE

Variable	Value
Brake fluid damping coefficient (C_{mc})	400 N.s/m
Master cylinder spring constant (K_{mc})	100 N/m
fuel-efficient area of the master cylinder piston (A_{mc})	0.448 m^2
Brake fluid bulk modulus (B_{mc})	12154.625 N/m^2
Master cylinder volume (V_{mc})	0.001 m^3
Master cylinder piston and brake fluid mass (M_{mc})	0.5 kg
Cross-sectional area of the caliper piston (A_{cal})	4.48 × 10^{-4} m^2
Brake caliper radius (R_{cal})	0.064 m
Brake pad friction coefficient (u_{pad})	0.4
Brake fluid time lag (t_b)	0.05 s
Flow resistances between the dynamic chamber and atmospheric air (C_{aa})	5.8 × 10^{-5} m.s
Flow resistances between the constant pressure chamber and the accumulator (C_{vm})	1.26 × 10^{-4} m.s
Ideal gas constant (R)	287.05 N.m/kg.K
Temperature (T)	300 K
Volume of the constant chamber (V_{vo})	2.4 × 10^{-3} m^3
Volume of dynamic chamber (V_{ao})	4.3 × 10^{-4} m^3
Brake booster diaphragm area (A_d)	0.053 m^2
Flywheel and shaft polar moment of inertia [$J(m_{el})$]	2.197 kg.m^2
Overall gear ratio (G)	6.67
Effective tire radius (r_t)	0.353 m
Mass of vehicle/assumption (M_v)	784.44 kg
Discrete-time step (T_s)	10^{-5}

Mechanical braking torque generated based on the brake pedal style signal is shown in Fig. 16. Mechanical braking torque is active at t = 7.08 s with initial T_{mech} = 0.274 Nm. Whereas the active brake pedal style signal at t = 7 s where the mechanical braking torque profile has a delay of 0.08 s. At t = 7.08 s to t = 7.68 s braking torque has increased reaching T_{mech} max (t = 7.68 s) = 125 Nm and at t = 9.64 s until t = 10 s has a significant decrease in torque reaching 24.57 Nm. The process of providing braking torque cannot be carried out together when providing acceleration to the actual state.

Fig. 17 shows the results of motor torque from the control system. From this picture, it can be seen that as long as the motor torque is negative, the motor is in the motoring mode. The transition from motoring to regenerative braking (generating mode) occurs very smoothly. It is important to realize that regenerative braking torque is not large enough to do all braking even at high flywheel speeds. The reason for the lack of regenerative braking torque is that motor power ratings are selected based on acceleration and not braking. This produces a system that will not fully use the regenerative braking capacity of ultracapacitors and thus will lose some regenerative braking efficiency. The minimum point of motor torque is T_{elec} min (t = 1.5 s) = -108.4 Nm while the maximum point is T_{elec} max (t = 7.96 s) = 34.22 Nm. Regenerative braking starts at t = 7.08 s.

Fig. 18 shows the results of the total braking torque expected from the actual braking torque from the simulation. The results show that the actual total braking torque tracks the control signal very well. Combining mechanical and regenerative braking torque is achieved smoothly. The max T_b value (t = 7.72 s) = 160.8 Nm, the ripples on this profile that occur between t = 7.72 s to t = 9.64 s are generated from mechanical braking ripples. The transition from motoring mode to generating mode occurs at t = 7.08 s. At this moment the torque value changes in a positive direction to carry out mechanical and regenerative braking processes.

A. *Simulation Results of Effects of Inertial Variations*

The simulation process is also carried out with variations in the inertia of the flywheel. This aims to determine the effect of differences in the equivalent mass of vehicles m_{e1} and m_{e2} as in Table 3.1 if using braking force, the parameter values of the motor, and the same ultracapacitor. Acceleration at the flywheel with the same initial energy value. Fig. 19 shows the simulation results of the effect of inertial variation on SOC of ultracapacitor stack.

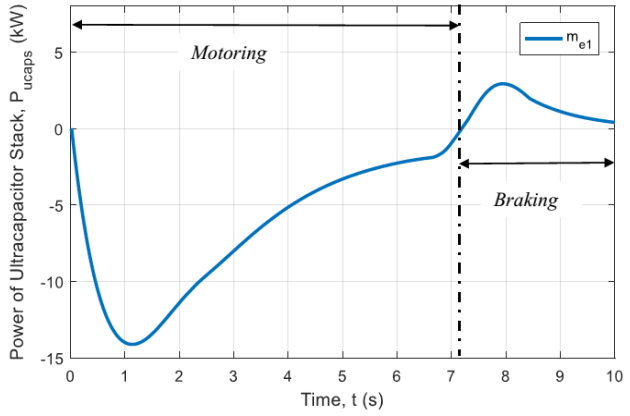

Fig. 14. Electric power flow on the ultracapacitor stack

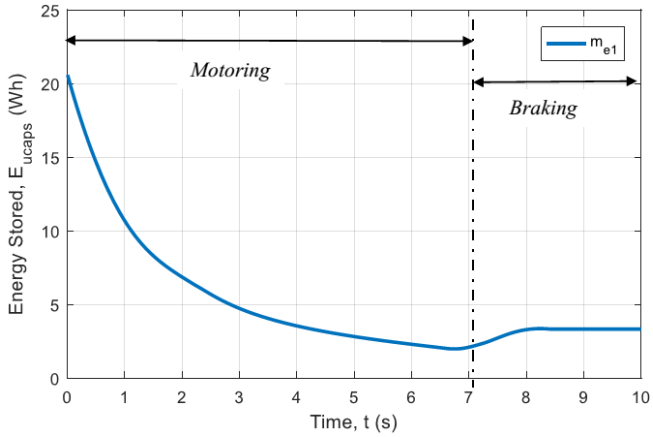

Fig. 15. Energy flow on the ultracapacitor stack

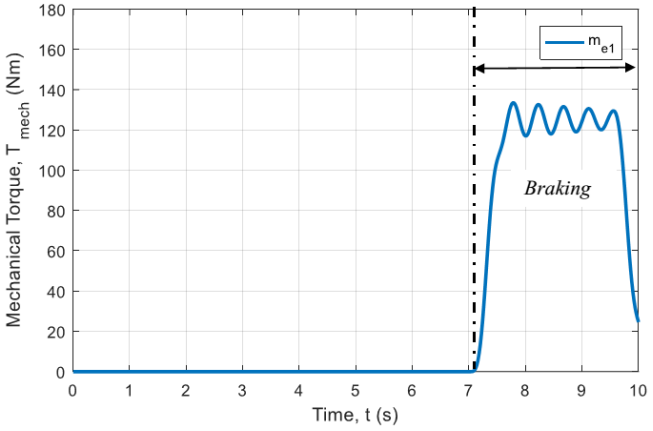

Fig. 16. Mechanical braking torque

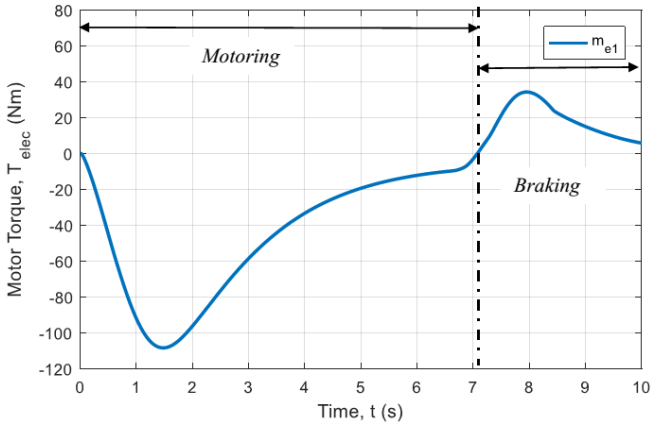

Fig. 17. Braking torque by the motor

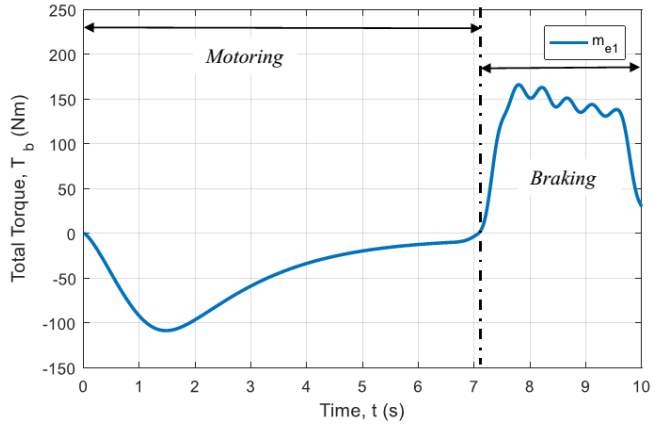

Fig. 18. Total braking torque

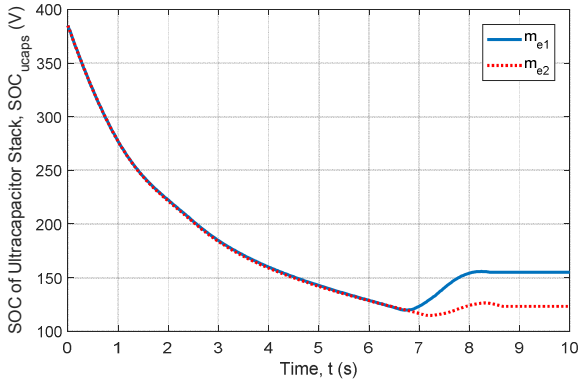

Fig. 19. SOC on ultracapacitor at two different vehicle masses

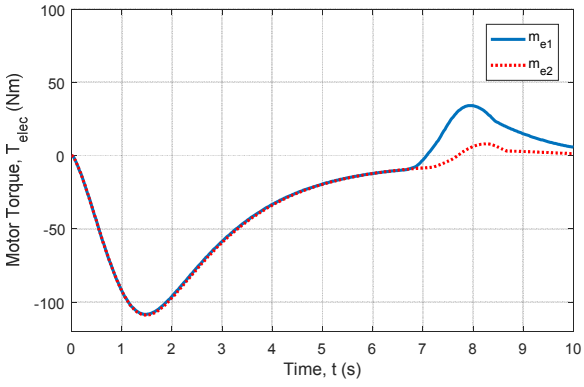

Fig. 20. Braking torque applied by the motor at two different vehicle mass

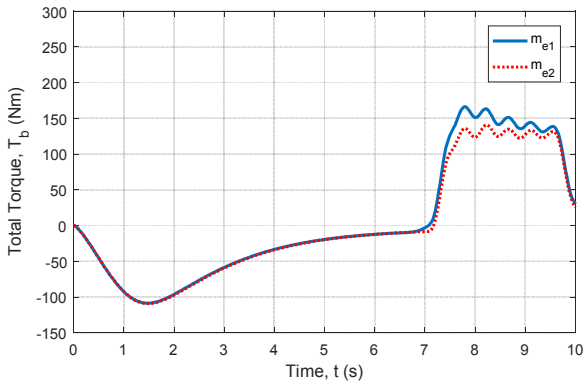

Fig. 21. Total braking torque at two different vehicle mass

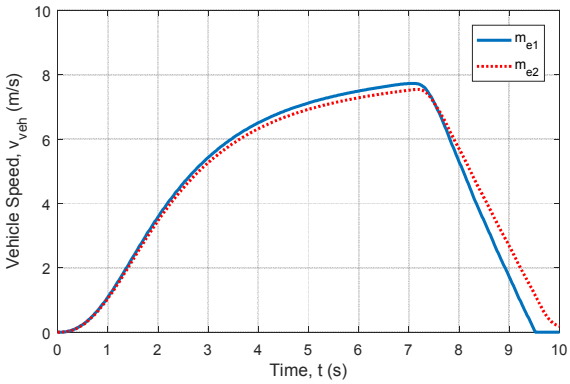

Fig. 22. Linear speed ratio of vehicles at two different vehicle mass

If the simulation on the flywheel is analogous to the linear velocity of the vehicle using a variation of the equivalent mass value, a plot of linear velocity differences and their effects is shown as regenerative and mechanical braking as shown in Fig. 22.

Regenerative braking efficiency can be calculated using Equation 10 [6], where $SOC_{initial}$ is the initial state of charge, SOC_{final} is the final state of charge, and SOC_{lowest} is the lowest state of charge. with a value of $\eta_{regen\ (m_{e1})}$ greater than $\eta_{regen\ (m_{e2})}$.

$$\eta_{regen} = \frac{SOC_{final} - SOC_{lowest}}{SOC_{initial} - SOC_{lowest}} \qquad (10)$$

Fig. 20 shows the effect of inertial variation on braking torque applied by the motor to the flywheel with the same braking force.

With the same mechanical braking force the total braking torque value depends on the variable braking torque applied by the motor as shown in Fig. 21.

B. Comparison of Regenerative and Non-Regenerative Braking Results

Simulation results without regenerative use the same model with regenerative but regenerative braking system is completely shut down and the braking is fully carried out by the mechanical brake, in other words, there is only one substrate on Stateflow namely Friction only Substrate.

Fig. 23 shows the results of the regenerative and without the regenerative braking comparison of SOCucaps values. At No Regen there is no increase in SOC_{ucaps} because there is only one braking condition, namely Friction only Substrate produces an output value y = 0 which means turning off the input value for Ideal Switch so that the electric current cannot flow back to the ultracapacitor stack when generating or when brake pedal pressed. Simulation is done with m_e value 1.

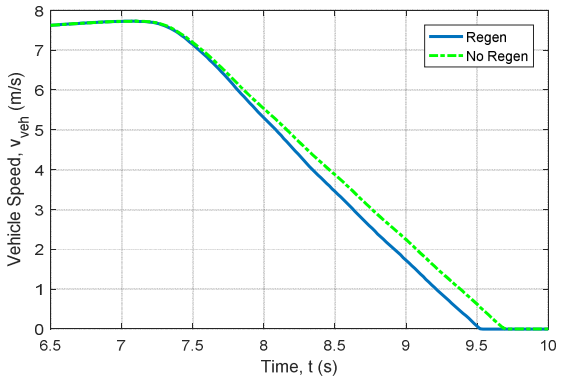

Fig. 23. The effect of regenerative braking to vehicle speed

V. CONCLUSION

In this paper, regenerative braking uses a parallel method has been modeled and simulated starting at the motor is in motoring mode such that the SOC of the ultracapacitor stacks will decrease exponentially from 385 V to 119.8 V. Furthermore, the simulation shows the case of the brake pedal is active causing the motor to operate in generating mode such that the SOC of the ultracapacitor stack has a linear increase from 119.8 V to 154.2 V.

In the study at two different vehicle mass, it can be observed that the increase in the vehicle mass results in the vehicle's travel time take 0.5 s longer and the regenerative braking efficiency value at 8.95% lower. The profiles of electric power flow, energy flow, mechanical braking torque, braking torque by the motor, and the State of Charge (SOC) of the ultracapacitor stacks have been presented during motoring and generating modes to show the effect of changing vehicle masses.

ACKNOWLEDGMENT

This paper was supported by USAID through Sustainable Higher Education Research Alliances (SHERA) Program-Centre for Collaborative Research (CCR) National Center for Sustainable Transportation Technology (NCSTT).

REFERENCES

[1] M, Ehsani., Y, Gao., S.E, Gay., dan A, Emadi. (2003). Modern Electric, Hybrid Electric, and Fuel Cell Vehicles - Fundamentals, Theory, and Design. Boca Raton, Florida: CRC Press, Ltd.. Trans. Roy. Soc. London, vol. A247, pp. 529–551, April 1955. *(references)*

[2] Krishnan, R. (2001). Electric Motor Drives: Modeling, Analysis, and Control. New Jersey: Prentice Hall, Inc.

[3] Todd, Philip. C. (2001). Snubber circuits: Theory, design, and application. Technical report, Texas Instruments Incorporated.

[4] Michael, Westbrook. (2001). The Electric Car: Development and Future of Battery, Hybrid and Fuel-Cell Cars. London, England: The Institution of Engineering and Technology.

[5] Miller, John. M. (2010). Propulsion Systems for Hybrid Vehicles. 2nd ed. London, England: The Institution of Engineering and Technology.

[6] Demers, Steven M. (2008). Mechanical and Regenerative Braking Integration for a Hybrid Electric Vehicle. Tesis. The University of Waterloo.

[7] Gerdes, J. C., dan Hedrick, J. Karl. (1999). Brake System Modeling for Simulation and Control. ASME, 121. 496..

[8] M, C. Wu., dan M, C. Shih. (2003). Simulated and Experimental Study of Hydraulic Anti-Lock Braking System Using Sliding-Mode PWM Control. Mechatronics, 13: 331-351.

[9] Panagiotidis, M., Delagrammatikas, G., dan Assanis, D. (2000). Development and Use of A Regenerative Braking Model for a Parallel Hybrid Electric Vehicle. SAE Technical Paper Series, 01-0995.

[10] Fajri, Poria., Ahmadi, Reza., dan Ferdowsi, Mehdi. (2012). Equivalent Vehicle Rotational Inertia Used for Electric Vehicle Test Bench Dynamic Studies. IEEE. 4115-4120

[11] Liu, Qinghe., Qu, Fufan., dan Song, Ji. (2017). A Novel Dual Function Pneumatic Valve for Blending Braking System and Control Strategies. IEEE. 255-261

[12] Rashid, M.H. (2011). Power Electronics Handbook: Devices, Circuits, and Applications Handbook. USA: Butterworth-Heinemann

[13] Qiu, Chengqun., Wang, Guolin., dan Meng, Mingyu. (2018). A novel control strategy of regenerative braking system for electric vehicles under safety critical driving situations. Energy.

[14] Prince, Agna., Abraham, Peter K., dan Aryanandiny. (2018). Design and Implementation of Ultra Capacitor Based Regenerative Braking System for a DC Motor. IEEE.

[15] Bhurse, Sneha S., dan Bhole, A.A. (2018). A Review of Regenerative Braking in Electric Vehicles. IEEE. 363-367.

[16] Naseri, Farshid., Farjah, Ebrahim., dan Ghanbari, Teymoor. (2016). An Efficient Regenerative Braking System Based on Battery/Supercapacitor for Electric, Hybrid and Plug-In Hybrid Electric Vehicles with BLDC Motor. IEEE.

[17] Sandilya, Debajit Kumar., dan Kalita, Bubumani. (2017). A study on Regenerative braking system with matlab simulation. IEEE.

[18] Mohan, Binesh., dan V.R, Bindu. (2018). Energy Regeneration in Induction Machine Drive during Braking. IEEE. 91-95.